7-1999

Core-Binding Factor Influences the Disease Specificity of Moloney Murine Leukemia Virus

Amy F. Lewis
Dartmouth College

Terryl Stacy
Dartmouth College

William R. Green
Dartmouth College

Lekidelu Taddesse-Heath
National Institutes of Allergy and Infectious Disease

Janet W. Hartley
National Institutes of Allergy and Infectious Disease

See next page for additional authors

JOURNAL OF VIROLOGY, July 1999, p. 5535–5547 Vol. 73, No. 7
0022-538X/99/$04.00+0

Core-Binding Factor Influences the Disease Specificity of Moloney Murine Leukemia Virus

AMY F. LEWIS,[1] TERRYL STACY,[1] WILLIAM R. GREEN,[2] LEKIDELU TADDESSE-HEATH,[3] JANET W. HARTLEY,[3] AND NANCY A. SPECK[1]*

Department of Biochemistry[1] and Department of Microbiology,[2] Dartmouth Medical School, Hanover, New Hampshire 03755, and Laboratory of Viral Diseases, National Institutes of Allergy and Infectious Disease, Bethesda, Maryland 20205[3]

Received 21 December 1998/Accepted 26 March 1999

The core site in the Moloney murine leukemia virus (Moloney MLV) enhancer was previously shown to be an important determinant of the T-cell disease specificity of the virus. Mutation of the core site resulted in a significant shift in disease specificity of the Moloney virus from T-cell leukemia to erythroleukemia. We and others have since determined that a protein that binds the core site, one of the core-binding factors (CBF) is highly expressed in thymus and is essential for hematopoiesis. Here we test the hypothesis that CBF plays a critical role in mediating pathogenesis of Moloney MLV in vivo. We measured the affinity of CBF for most core sites found in MLV enhancers, introduced sites with different affinities for CBF into the Moloney MLV genome, and determined the effects of these sites on viral pathogenesis. We found a correlation between CBF affinity and the latent period of disease onset, in that Moloney MLVs with high-affinity CBF binding sites induced leukemia following a shorter latent period than viruses with lower-affinity sites. The T-cell disease specificity of Moloney MLV also appeared to correlate with the affinity of CBF for its binding site. The data support a role for CBF in determining the pathogenic properties of Moloney MLV.

Murine leukemia viruses (MLVs) are replication-competent retroviruses, some of which induce leukemias and lymphomas when injected into newborn mice. Both viral and host genetic factors influence the leukemogenicity of MLVs and their disease specificities. One determinant of MLV pathogenesis is the viral transcriptional enhancer. Enhancers can influence the tissue tropism of an MLV, the rate of disease onset, and disease specificity. For example, the SL3-3 MLV, a thymotropic, highly leukemogenic virus, has a potent transcriptional enhancer that significantly influences pathogenesis by this virus. Replacement of the SL3-3 enhancer (U3 region) with that from the weakly leukemogenic Akv virus converts SL3-3 MLV into an essentially nonpathogenic virus (36). Another well-studied example is the enhancer from the Moloney MLV, which determines the selectivity of the Moloney virus for inducing T-cell lymphomas. Substitution of the Moloney virus enhancer with that from the erythroleukemogenic Friend MLV switches the disease specificity of Moloney MLV from T-cell lymphoma to erythroleukemia (9, 10, 22, 31, 38).

An abundance of transcription factor binding sites have been found in MLV enhancers, several of which influence MLV pathogenesis. One site that has received considerable attention is the so-called core site, which was shown to contribute to the pathogenic properties of both the Moloney and SL3-3 MLVs. Mutation of the core site in Moloney MLV significantly altered the disease specificity of Moloney MLV from T-cell lymphoma to erythroleukemia (70). In SL3-3 MLV, core site mutations had different effects, depending upon the particular base pair change that was introduced and the number of core sites mutated. Some mutations increased the latent period of disease onset by SL3-3, while others almost completely attenuated pathogenesis by the virus (1, 27, 47). SL3-3 MLV enhancers containing core site mutations often accumulated secondary mutations in vivo that restored some amount of transcriptional activity to the enhancer and pathogenic potential to the virus (17, 18, 47).

We and others identified and purified a protein that binds the SL3-3 and Moloney MLV core sites and named it CBF (for core-binding factor) (33, 40, 69, 78, 82). We purified CBF from calf thymus based on its ability to bind the wild-type Moloney MLV core site but not the mutated core site that shifted disease specificity of Moloney MLV to erythroleukemia (70, 82). CBF was independently purified based on its binding to the polyomavirus enhancer and is also known as the polyomavirus enhancer binding protein 2 (PEBP2) (33).

Numerous studies have underscored the importance of CBF in hematopoiesis. CBF is a heterodimer consisting of a DNA-binding subunit called CBFα and a non-DNA-binding subunit, CBFβ (33, 54, 55, 83). Three related genes encode CBFα subunits (*Cbfa1*, *Cbfa2*, and *Cbfa3*), and one gene encodes the common CBFβ subunit (*Cbfb*) (2, 3, 37, 39, 46, 54, 55, 83). Homozygous disruption of two of the CBF genes in mice, *Cbfa2* and *Cbfb*, blocks fetal liver hematopoiesis (48, 56, 64, 80, 81). All definitive hematopoietic lineages are affected by the *Cbfa2* and *Cbfb* mutations, suggesting that *Cbfa2* and *Cbfb* are required at the level of the pluripotent hematopoietic stem cell. In addition, mutations in the human *Cbfa2* and *Cbfb* homologues (*CBFA2* [also known as *AML1*] and *CBFB*) are associated with leukemias in humans. The *CBFA2* gene is the target of the t(8;21)(q22;q22) associated with 15% of de novo acute myeloid leukemias (5, 46), the

* Corresponding author. Mailing address: Department of Biochemistry, Dartmouth Medical School, Hanover, NH 03755. Phone: (603) 650-1159. Fax: (603) 650-1128. E-mail: Nancy.A.Speck@dartmouth.edu.

t(12;21)(p13;q22) found in 30% of pediatric de novo acute lymphocytic leukemias (24, 42, 61, 62, 66), and the relatively rare t(3;21)(q26;q22) and t(16;21)(q24;q22) found in therapy-related leukemias and myelodysplasias (20, 52, 53). The *CBFB* gene is disrupted in approximately 15% of acute myeloid leukemias by inv(16)(p13;q22), t(16;16), and del(16)(q22) (39, 67). CBF binds a number of cellular genes transcribed in hematopoietic cells, including genes encoding the T-cell receptor α, β, γ, and δ chains (TCRα, TCRβ, TCRγ, and TCRδ, respectively), immunoglobulin μ chain, interleukin 3, granulocyte/monocyte colony-stimulating factor, CD3ε, myeloperoxidase, neutrophil elastase, and granzyme B serine protease (8, 16, 19, 21, 28, 30, 51, 59, 60, 76, 84, 87).

The importance of CBF in hematopoietic cells makes it a strong candidate for the factor that contributes to the leukemogenic properties of MLVs in vivo. However, CBF is not the only transcription factor that binds the Moloney and SL3-3 MLV core sites in vitro. Activating protein 3 (AP-3), mammalian C-type retrovirus enhancer factor 1 (MCREF-1), and SL3 core-binding factor (S-CBF) also bind MLV core sites (40, 41, 44, 75), and there may be other core-binding factors not yet identified. To address the question of whether CBF is the relevant core-binding factor for Moloney MLV pathogenesis in vivo, we considered two approaches. One approach is to eliminate or overexpress CBF in mice and determine whether modification of CBF levels affects pathogenesis by Moloney MLV. However, an inherent difficulty with this approach is that hematopoiesis itself may be severely perturbed by anomalous levels of CBF. This is certainly the case when CBFα2 or CBFβ is eliminated entirely, which severely impairs hematopoiesis, resulting in embryonic lethality (48, 56, 64, 80, 81). Overexpression is also likely to be problematic, as evidenced by the recent discovery that *Cbfa1* is a preferential proviral insertion site in lymphomas induced by Moloney MLV in c-*myc* transgenic mice (72).

An alternative approach, and the tack we chose to follow, is to systematically modify the affinity of CBF for the core site in the Moloney MLV enhancer by altering the nucleotide composition of the site. Our hypothesis was that if CBF is the relevant core-binding factor for Moloney MLV pathogenesis in vivo, we should observe a correlation between the affinity of CBF for its site and the latent period of disease onset, and/or the disease specificity of the virus. To this end, we measured the affinity of CBF for a large panel of naturally occurring and synthetic core sites. We identified core sites whose affinities for CBF span 5 orders of magnitude, engineered those sites into the Moloney MLV genome, and examined their impact on pathogenesis by Moloney MLV. We observed a relationship between CBF affinity and the latent period of disease onset, in that Moloney MLVs with high-affinity CBF binding sites induced leukemia or lymphoma with a shorter latent period than viruses with low-affinity sites. Disease specificity also correlated with the affinity of CBF for its site, supporting a role for CBF in Moloney MLV pathogenesis.

MATERIALS AND METHODS

Expression and purification of the CBFα2 Runt domain. A DNA fragment encoding the DNA-binding (Runt) domain from the murine CBFα2 protein (amino acids 41 to 190) (3) was amplified by PCR using the following primers: 5′-CGGAATTCCCATATGGCCAGCAAGCTGAGGAGC-3′ (sense) and 5′-CGGGATCCTTACTCGTGCTGGTTCTTCCCGGGCTTGGTCTGATC-3′ (antisense). The antisense primer introduces a translational stop codon followed by codons for the amino acids KNQHE immediately 3′ to codon 190 of CBFα2. PCR products were digested with *Nde*I and *Bam*HI, subcloned into the corresponding sites of the pET-3c vector (Novagen, Madison, Wis.), and transformed into the *Escherichia coli* BL21(DE3)LysS for expression (74). A single colony was grown to an absorbance (A_{600}) of 0.3 to 0.4 in Luria-Bertani (LB) medium containing 100 μg of carbenicillin per ml and 50 μg of chloramphenicol per ml, and a glycerol stock was prepared.

All purification steps were performed at 4°C, unless otherwise noted. A scraping of the frozen bacterial stock was thawed at room temperature, and 1 μl was diluted into 1.0 ml of LB medium. A 1-μl aliquot of this 1:1,000 dilution was used to inoculate 1 liter of LB medium containing 100 μg of carbenicillin per ml and 50 μg of chloramphenicol per ml. The cells were grown for approximately 16 h at 37°C to an absorbance (A_{600}) of 0.3 to 0.4, and expression was induced with 1 mM isopropyl-β-D-thiogalactopyranoside (IPTG). Cells were harvested between 1 and 3 h postinduction by centrifugation at 4,800 × *g*. The bacterial pellet was resuspended in an equal weight of lysis buffer (10% sucrose, 50 mM Tris-HCl [pH 7.5], protease inhibitors [1 mM Pefabloc, 1 mM phenylmethylsulfonyl fluoride, 50 μM Calpain inhibitor 1, 1 μg of leupeptin per ml, 1 μg of pepstatin A per ml, 2 μg of aprotinin per ml] [Sigma]). The cells were dropped directly into liquid nitrogen, and frozen cell pellets were stored at −70°C or thawed immediately. Cells were thawed in a room temperature water bath, and ammonium sulfate was added to a final concentration of 0.1 M. The tube was inverted once and incubated on ice for 30 min. Cells were lysed at 37°C for 2.5 min and centrifuged at 40,000 × *g* for 1 h at 4°C. Soluble protein was collected, dialyzed against 200 volumes of buffer A (150 mM KCl, 20 mM imidazole [pH 7.0], 20 mM β-mercaptoethanol), and loaded onto a 20-cm^3 DEAE-Sephacel column (Pharmacia Biotech, Piscataway, N.J.) equilibrated in buffer A. The flowthrough fraction was collected, dialyzed against 200 volumes of buffer B (50 mM NaCl, 20 mM HEPES [pH 7.5], 20 mM β-mercaptoethanol, 10% glycerol, 0.05% Triton X-100), and applied to a P-11 phosphocellulose column (1.5 cm^3; Whatman), equilibrated in buffer B. The column was developed with a 22-ml linear gradient from 0.05 to 1.0 M NaCl in buffer B. Fractions containing the Runt domain were pooled and exchanged into buffer C (8 mM sodium phosphate [pH 7.5], 50 mM NaCl, 0.05% Triton X-100, 10% glycerol, 10 mM β-mercaptoethanol), and loaded onto a hydroxylapatite column (1 cm^3; HTP, Bio-Rad Laboratories, Richmond, Calif.). The hydroxylapatite column was developed with a 40-ml linear gradient from 8 to 200 mM sodium phosphate in buffer C, and fractions containing the Runt domain were pooled and stored at −70°C. The Runt domain concentration was determined by A_{280} with the molar extinction coefficient ε = 11,000 $M^{-1} \cdot cm^{-1}$ reported previously (12).

Determination of the active Runt domain concentration. The active Runt domain concentration was determined by titration of known concentrations of DNA onto a fixed concentration of the Runt domain, as described previously (12). The DNA site used in the titrations was derived from the TCRβ enhancer (GGATATATGTGGTTTGCA). Oligonucleotide concentrations were determined by measuring A_{260}, using extinction coefficients calculated with the Oligo program (National Biosciences, Inc.). One milliliter of a 1:15 dilution of [γ-^{32}P]ATP (7,000 Ci/mmol; ICN) was used to label 250 pmol of single-stranded oligonucleotide. A portion of the single-stranded DNA was set aside for quantitative purposes (see below), and the remainder of the labeled strand was annealed to an unlabeled complementary strand. All binding reactions and electrophoretic mobility shift assays (EMSA) were performed as described previously (12). Briefly, binding reactions (20 μl of total volume) were performed at 4°C for 20 min in a solution consisting of 10 mM Tris-HCl (pH 7.5), 100 mM NaCl, 1 mM EDTA, 5 mM dithiothreitol, 0.2 μg of bovine serum albumin per ml, 0.05% Triton X-100, and 4% glycerol. The Runt domain concentration in all reaction mixtures (5×10^{-8} M) was 100-fold above the K_d of the Runt domain for this particular DNA site, and the concentration of DNA was varied. Portions (15 μl) of the binding reaction mixtures were loaded onto a running gel (10% polyacrylamide) at 4°C to separate free DNA from protein-bound DNA. For each DNA concentration, three reaction mixtures were analyzed: (i) one with the Runt domain added, (ii) a control containing the double-stranded DNA probe alone, and (iii) the labeled single-stranded DNA of known concentration. The amount of free DNA in each lane was determined with a PhosphorImager 445SI Scanner (Molecular Dynamics, Sunnyvale, Calif.) and IPLab gel. [D_f], the concentration of free double-stranded DNA in lanes containing the Runt domain, and [D_t], the concentration of free double-stranded DNA in the corresponding control lane without added Runt domain, were determined by comparison to the free single-stranded DNA standard of known concentration. The concentration of bound DNA, [*PD*], was determined from the equation $[PD]/[D_t] = 1 - [D_f]/[D_t]$. Concentrations of active protein were determined from the asymptote when [*PD*] versus [D_t] was plotted.

Equilibrium dissociation constants. Equilibrium dissociation constants were determined by the method of Jonsen et al. (32), using the binding and EMSA conditions described above. DNA concentrations were at least 10-fold lower than the estimated K_d of the Runt domain for the DNA site, ensuring the total active protein concentration, [P_t], was an accurate estimate of free protein, [*P*]. The fraction of free DNA, $[D_f]/[D_t]$, was the ratio of the free DNA signal analyzed at each protein concentration to the DNA signal in a control lane containing no protein. The fraction of DNA in complex with protein was derived from the equation $[PD]/[D_t] = 1 - [D_f]/[D_t]$. All datum points were fit to the rearranged mass action equation, $[PD]/[D_t] = 1/(1 + K_d/[P])$, using nonlinear least-squares analyses (Kaleidagraph; Synergy Software).

Sequences of the double-stranded binding sites used to measure the equilibrium dissociation constants are listed on the next page.

Moloney MLV	5′-GGATATCTGTGGTAAAGCA-3′ 3′-CCTATAGACACCATTTCGT-5′
SL3-3 MLV	5′-GGATATCTGTGGTTAAGCA-3′ 3′-CCTATAGACACCAATTCGT-5′
Akv	5′-GGATATCTGTGGTCAAGCA-3′ 3′-CCTATAGACACCAGTTCGT-5′
MCF247	5′-GGATATCTGTGGTCGAGCA-3′ 3′-CCTATAGACACCAGCTCGT-5′
Rauscher MCF	5′-GGATATCTGCGGTGAGCA-3′ 3′-CCTATAGACGCCACTCGT-5′
MX	5′-GGATATCGGTGGTCAAGCA-3′ 3′-CCTATAGCCACCAGTTCGT-5′
Soule MLV	5′-GGATATCTGCGGTCAGCA-3′ 3′-CCTATAGACGCCAGTCGT-5′
TCRα	5′-GGATATATGTGGCTTGCA-3′ 3′-CCTATATACACCGAACGT-5′
TCRβδ	5′-GGATATATGTGGTTTGCA-3′ 3′-CCTATATACACCAAACGT-5′
TCRγ	5′-GGATATCTGTGGTTTGCA-3′ 3′-CCTATAGACACCAAACGT-5′
HA	5′-GGATATTTGCGGTTAGCA-3′ 3′-CCTATAAACGCCAATCGT-5′
SAAB	5′-GGATATCTGCGGTTTGCA-3′ 3′-CCTATAGACGCCAAACGT-5′
SS4	5′-GGATATCTGCGGAAGGCA-3′ 3′-CCTATAGACGCCTTCCGT-5′
SS5	5′-GGATATCTGTGGAAGAGCA-3′ 3′-CCTATAGACACCTTCTCGT-5′
Mo(core)	5′-GGATATCTGCCGTAAAGCA-3′ 5′-CCTATAGACGGCATTTCGT-5′

Plasmids and mutations. DNA fragments used for subcloning were derived from the plasmids pMoCAT, pMo(CORE)CAT, and pMoΔRVCAT. pMoCAT contains the wild-type Moloney MLV enhancer linked to the bacterial chloramphenicol acetyltransferase (CAT) gene, and pMo(CORE)CAT is the same plasmid with mutations in both core sites of the Moloney MLV enhancer that reduce CBFα2 binding by 1,000 fold (71; this study). pMoΔRVCAT lacks the *Eco*RV-*Eco*RV fragment within the enhancer direct repeat. From these initial plasmids, four additional vectors were made: pMoRV (Fig. 1) contains the *Eco*RV-*Eco*RV enhancer fragment from pMoCAT, subcloned into the *Eco*RV site of pBluescript SK+ (Stratagene). pMoLUC, pMoΔRVLUC, and pMo(CORE)LUC contain a *Sau*3AI-*Kpn*I fragment from the Moloney MLV U3/R region subcloned into the *Bam*HI-*Kpn*I site of the pxp1 vector, a promoterless vector containing the firefly luciferase gene (LUC) (14, 49).

The strategy for introducing core site mutations into the Moloney enhancer is illustrated schematically in Fig. 1. Mutations were made by PCR, using primers with the following sequences (core sites are underlined, and lowercase letters indicate the mutated nucleotides), in conjunction with an antisense primer (LUC) from luciferase coding sequences: Soule (sense), 5′-CAGGATATCTGcGGTcAGCAGTTCC-3′; SL3-3 (sense), 5′-CAGGATATCTGTGGTtAGCAGTTCCT-3′; MX (sense), 5′-CAGGATATCgGTGGTcAGCAGTTCC-3′; SS4 (sense), 5′-CAGGATATCTGcGGaAgGCAGTTCCTG-3′; SS5 (sense), 5′-CAGGATATCTGTGGaAgGCAGTTCCTG-3′; and LUC (antisense), 5′-CCGGGCCTTTCTTTATGT-3′.

All core site sequences were terminated at the 5′ and 3′ ends of the CBF phosphate contacts defined previously (underlined) (43). Core sequences were fused directly to Moloney MLV flanking sequences in such a way as to maintain the orientation and spacing of other protein binding sites on the Moloney enhancer. Mutations were introduced into each copy of the direct repeat in two separate subcloning steps. First, each sense primer was used with the LUC1 antisense primer and pMoΔRVLUC as a template in PCRs that amplified from nucleotide 8029 of the Moloney MLV genome to nucleotide 86 of the luciferase gene. The PCR products were digested with *Eco*RV and *Kpn*I, and isolated fragments were used to replace the corresponding region in pMoΔRVCAT to create the pMo(*)ΔRVCAT vectors [pMo(Soule)ΔRVCAT, pMo(SL3)ΔRVCAT, pMo(MX)ΔRVCAT, pMo(SS4)ΔRVCAT, and pMo(SS5)ΔRVCAT] (Fig. 1A). Core site mutations were independently introduced into the 75-bp *Eco*RV-*Eco*RV fragment of the Moloney enhancer by PCR using pMoRV as a template and the same sense primers in conjunction with an antisense primer that hybridizes to the T7 promoter in the pBluescript SK+ vector. The PCR products were digested with *Eco*RV and subcloned into the *Eco*RV site of the pMo(*)ΔRVCAT vectors, generating pMo(*)CAT vectors with identical core site mutations in both copies of the Moloney MLV enhancer direct repeat [pMo(Soule)CAT, pMo(SL3)CAT, pMo(MX)CAT, pMo(SS4)CAT, and pMo(SS5)CAT] (Fig. 1B). Finally, these mutated Moloney enhancers were excised from the pMo(*)CAT plasmids with *Sau*3A1 and *Kpn*I and transferred into the *Bam*HI-*Kpn*I sites of the firefly luciferase vector (pxp1) to generate pMo(Soule)LUC, pMo(SL3)LUC, pMo(MX)LUC, pMo(SS4)LUC, and pMo(SS5)LUC (Fig. 1C). The correct sequence of all enhancer segments generated by PCR was confirmed.

Substitution of the mutated Moloney MLV enhancers into the infectious Moloney MLV genome was performed as described previously (70).

Cell lines. Cell lines were used in transfection experiments or for the generation of infectious virus as follows. A human mature T-cell line (Jurkat) and a murine pro-T-cell line (2017) were maintained in RPMI 1640 supplemented with 10% fetal bovine serum (FBS), 100 U of penicillin per ml, 100 μg of streptomycin per ml, and 2 mM L-glutamine. A murine mature T-cell line, D5H3, was maintained in Dulbecco modified Eagle medium supplemented with 10% FBS, 100 U of penicillin per ml, 100 μg of streptomycin per ml, 2 mM L-glutamine, 0.01 M HEPES (pH 7.9), and 5 mM β-mercaptoethanol. After transfection, D5H3 cells were transferred into the same medium with 5% FBS and 5% newborn bovine serum. NIH 3T3 cells were maintained in Dulbecco modified Eagle medium with 10% FBS, 2 mM L-glutamine, and antibiotics.

Luciferase assays. Cells were transfected by the DEAE-dextran method (34). Briefly, 10^7 Jurkat and 2017 cells or 5×10^6 D5H3 cells were transfected with 5 μg of the Mo(*)LUC reporter plasmids and 5 μg of CMVhGH, a plasmid containing cDNA encoding the human growth hormone driven from a cytomegalovirus enhancer (Nichols Institute Diagnostics, San Juan Capistrano, Calif.). Jurkat cells were induced with 1 μg of 1,3-phorbol myristate acetate per ml at 24 h posttransfection. Cells were harvested 48 h posttransfection, washed once with phosphate-buffered saline, and lysed in 160 μl of lysis buffer (1% [vol/vol] Triton X-100, 25 mM glycylglycine [pH 7.8], 15 mM $MgSO_4$, 4 mM EGTA, 1 mM dithiothreitol) by vortexing for 30 s at room temperature. Supernatants were harvested and assayed immediately for luciferase enzyme activity (14, 25). The results were normalized against protein concentration and human growth hormone levels.

Generating infectious viruses. We transfected three independent molecular clones of each mutated viral genome into NIH 3T3 cells as previously described (70). Cells were split 1:10 into duplicate plates 8 to 12 h following transfection, and XC plaque assays were performed directly on one such plate (63). In all cases, XC plaques were present. The remaining plate was maintained for 2 weeks, at which time the culture supernatants were assayed for reverse transcriptase activity (4). Virus was harvested after 2 to 3 weeks, by which time the virus had spread throughout the culture, as determined by XC plaque assay.

Mice, tumor induction, and classification of disease. Newborn (<2-day-old) NFS mice were inoculated intraperitoneally and intrathymically with 0.04 ml of tissue culture-grown virus, representing from $10^{4.3}$ to $10^{5.3}$ PFU/mouse. Viruses from two or three independent molecular clones from each enhancer mutation were injected. Animals were monitored regularly for overt signs of disease. Diagnosis of erythroleukemia, lymphoma, or myelogenous leukemia was based on gross pathology and histology, as described previously (10). Briefly, diagnosis of lymphoblastic lymphoma was based on gross findings of enlarged thymus, lymph nodes, or both, and histological observation of diffuse infiltration with lymphoblasts of splenic white pulp, thymus, and lymph nodes, and often liver. Spleens were normally but not invariably enlarged. Spleen DNA from cases of lymphoblastic leukemia without thymic enlargement was analyzed for TCRβ and immunoglobulin heavy-chain (IgH) rearrangements by Southern blotting (26, 29, 35). Mice with erythroleukemia showed severe anemia and had enlarged spleens with erythroblast infiltration of expanded red pulp and enlarged livers with blast infiltration within sinusoids, the thymus was never enlarged, and lymph nodes were normal or showed enlarged germinal centers.

RESULTS

Expression and purification of the Runt domain. We used the isolated DNA-binding Runt domain from the murine CBFα2 protein to measure equilibrium dissociation constants for different core sites. Although the Runt domain's affinity for any given DNA site may differ from that of the full-length CBFα2-CBFβ heterodimer, its relative affinities for different core sites should be comparable to those of the full-length proteins. We expressed a fragment spanning amino acids 41 to 190 of CBFα2 that contains the Runt domain, plus additional sequences at the N and C termini of the Runt homology region that we found improved both expression in bacteria and DNA binding (unpublished results). We also added the pentapeptide KNQHE to the C terminus of the Runt domain that was shown to decrease degradation of the P22 Arc repressor in bacteria (7, 45, 57, 58). We purified the Runt domain from the soluble fraction of a bacterial cell lysate by sequential chromatography on DEAE-Sephacel, P11 phosphocellulose, and hydroxylapa-

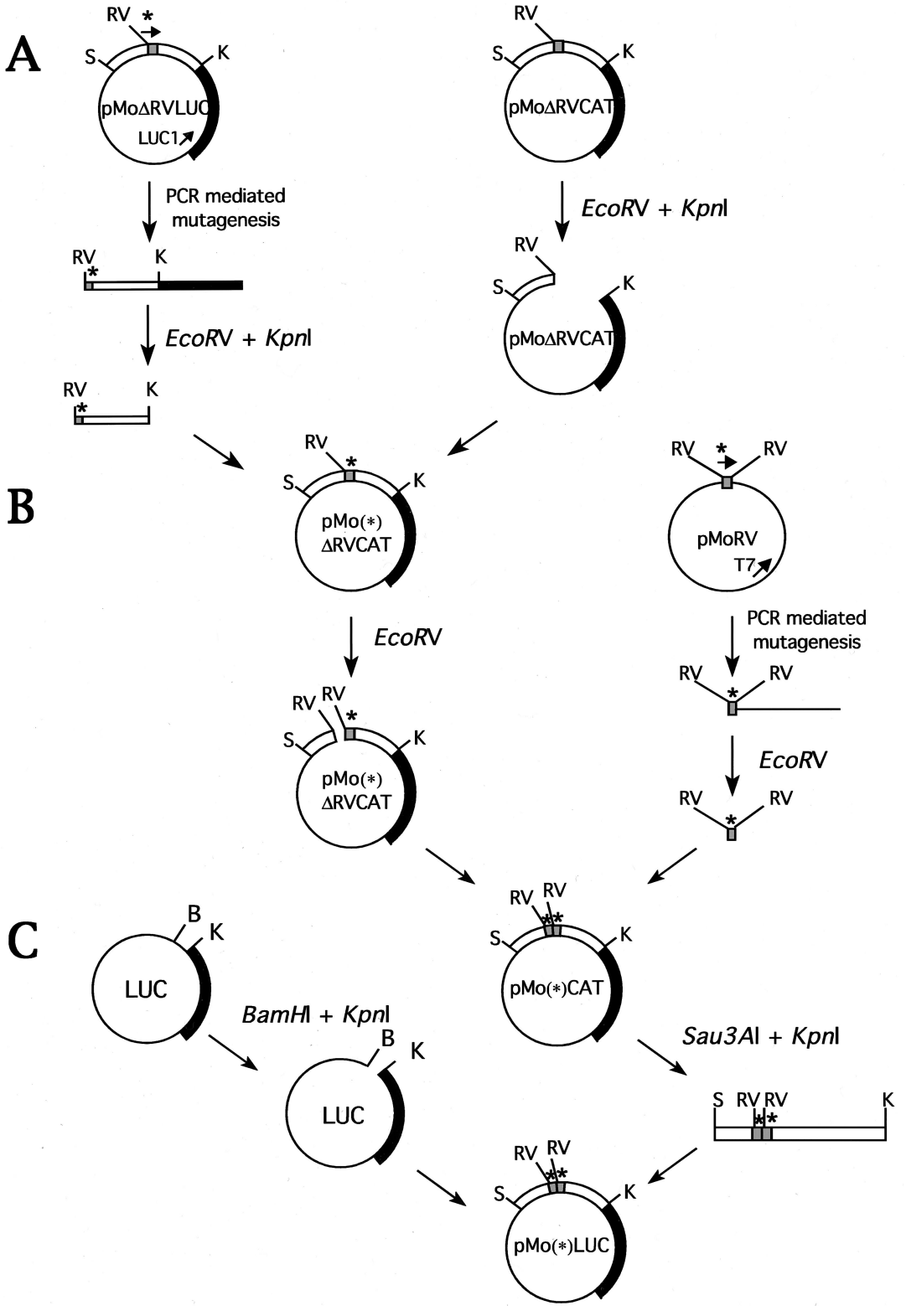

FIG. 1. Strategy for introducing altered core sites into the Moloney MLV enhancer. (A) Introducing point mutations into the promoter-distal copy of the enhancer direct repeats. White bars represent sequences from the Moloney MLV genome. Black bars represent sequences from the bacterial chloramphenicol acetyltransferase (CAT) gene or the luciferase gene (LUC). Black lines represent bacterial vector DNA sequences. A small gray square represents one copy of the 75-bp direct repeat. The PCR primer locations (arrows) and core site mutations (asterisks) are indicated. The luciferase reporter plasmid (pxp1) is a promoterless vector linked to the firefly luciferase gene (LUC) (14, 49). Abbreviations: B, *Bam*HI; RV, *Eco*RV; K, *Kpn*I; S, *Sau*3AI. (B) Introducing mutations into the promoter-proximal copy of the direct repeat. (C) Introducing mutated enhancers into the luciferase reporter vector. Sequences from *Sau*3AI$_{7910}$-*Kpn*I$_{8296}$ of Moloney MLV (85) encompass the 75-bp repeat and extend 30 bp 3′ to the viral cap site.

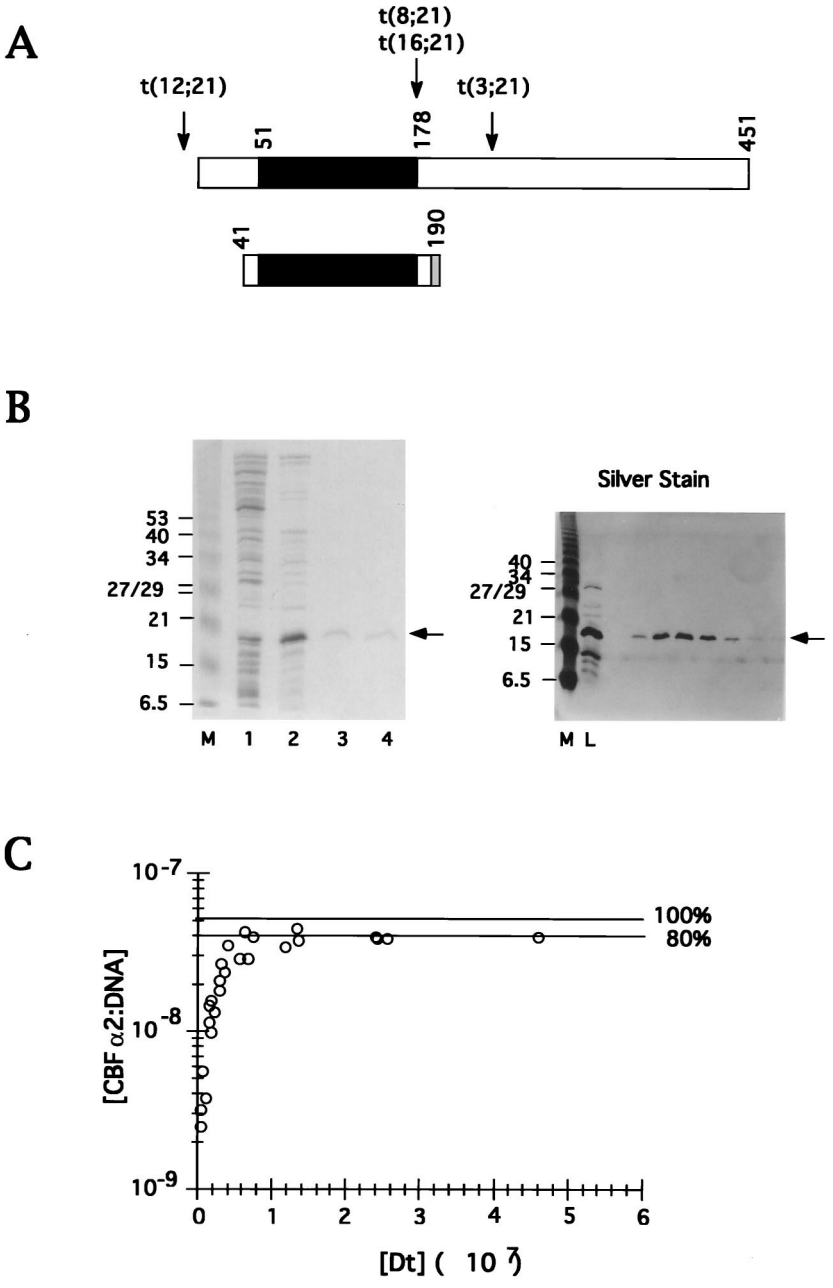

FIG. 2. Expression and purification of the CBFα2 Runt domain. (A) Schematic diagram of full-length CBFα2(451) (3) with the boundaries of the expressed Runt domain shown below. Black rectangles indicate the 128-amino-acid region of homology shared by the *Drosophila* and mammalian CBFα proteins. The t(8;21)(q22;q22), t(3;21)(q26;q22), t(16;21)(q24;q22), and t(12;21)(p13;q22) breakpoint locations are indicated by arrows. The KNQHE C-terminal tag is indicated by the gray bar. (B) Purification of the CBFα2 Runt domain. (Left) Coomassie brilliant blue-stained sodium dodecyl sulfate-polyacrylamide gel with active fractions from each step of the purification. Lanes: M, molecular markers (in kilodaltons); 1, soluble supernatant from crude bacterial cell lysate; 2, DEAE-Sephacel flowthrough fraction; 3, phosphocellulose eluate; 4, hydroxylapatite eluate. The arrow indicates the location of the CBFα2 Runt domain fragment. (Right) Silver-stained sodium dodecyl sulfate-polyacrylamide gel of representative active fractions (66 to 94) from the hydroxylapatite column. Lane L (for load) contains the phosphocellulose eluate. (C) Activity of the purified Runt domain quantified by DNA titration in an EMSA. Concentrations (molar) of protein-DNA complex [PD] versus total input DNA [D_t] are plotted.

tite, as described in Materials and Methods, and summarized in Fig. 2 and Table 1. The overall yield of the protein was 20%, and the estimated purity was >95%.

We determined the concentration of Runt domain active for DNA binding by titrating DNA of known concentration onto protein of unknown active concentration until saturation of protein with DNA was achieved (Fig. 2C). The percent active protein was approximated from the asymptote of the curve that resulted from plotting the total concentration of DNA versus the concentration of protein-DNA complex. The purified Runt domain was estimated to be 80 to 100% active compared to the total protein concentration.

Equilibrium dissociation constants of the Runt domain for various core sites. We measured the affinity of the Runt do-

TABLE 1. Purification of the CBFα2 Runt domain[a]

Amt (mg) of:		Fold purification	Total yield (%)
Total protein[b]	Runt domain[c]		
92.5	5.65		100
12.3	1.86	2.46	33
2.80	1.69	9.87	30
1.11	1.11	16.37	20

[a] Data are for a single preparation starting with a 4-liter bacterial culture.
[b] Protein was measured by Bio-Rad DC protein assay with bovine serum albumin as a standard.
[c] Runt domain was quantified by Coomassie brilliant blue staining of a sodium dodecyl sulfate-polyacrylamide gel.

main for different core sites (Table 2) by equilibrium binding analysis, using the EMSA. The core sites tested were derived from MLV enhancers (23, 73), the TCRα, -β, -γ, and -δ enhancers (21, 30, 59, 60), and five synthetic sites. The five synthetic sites include the high-affinity (HA) site identified by Thornell et al. (77), a site identified by selected and amplified binding analysis (SAAB) (43), a site containing an A at position 7 known to decrease CBF binding (SS4) (33), a site similar to SS4 that incorporates a C→T transition at the fourth position (SS5), and the original mutant core site, Mo(core), that altered disease specificity of Moloney MLV from T-cell leukemia to erythroleukemia (70). All core sites were flanked at the 5′ and 3′ ends with sequences derived from the Moloney MLV enhancer. Affinities of the CBFα2 Runt domain for different core sites were determined by titrating purified Runt domain of known active concentration onto DNA at a concentration at least 10-fold lower than the K_d of the Runt domain for that site. The Runt domain-DNA complex was separated from free DNA by EMSA, and the ratio of Runt domain (CBFα)-DNA complex to total DNA (D_t) was then plotted against the active concentration of the Runt domain to obtain a K_d value (Fig. 3 and Table 3).

The equilibrium dissociation constants of the CBFα2 Runt domain for the core sites tested spanned 5 orders of magnitude. We organized the sites into six groups (Table 3). Group I contains the highest-affinity sites and includes the site identified by selected and amplified binding analysis (CTGCGGTTT) (43), and the original high-affinity site identified by Thornell et al. (TTGCGGTTA) (77). Group I also includes the core site from the Soule MLV enhancer (CTGCGGTCA). All three high-affinity sites contain a C in the fourth position (underlined in each site). Values obtained with the Soule MLV core site fluctuated from one experiment to the next for unknown reasons. Thus, data from six separate experiments were plotted on one graph to obtain the best possible K_d estimate for the Soule site (Fig. 3).

The core sites in the Moloney, SL3-3, and Akv enhancers fell into the second highest affinity group (Table 3, group II). The group II sites had, on average, a 10-fold-lower affinity for the Runt domain than the group I sites. All of the group II sites, except for the Rauscher MLV site, possess a T in the fourth position, as opposed to the C found in the highest-affinity group I sites. The Runt domain affinities for the Moloney and SL3-3 MLV core sites were equivalent. The Runt domain affinity for the Akv core site was less than twofold lower than for the SL3-3 MLV site, consistent with previously published data (86).

Group III sites include the TCRα and -β core sites, and the site found in the endogenous polytropic MX33 and MX27 viruses (MX). Both the TCRα and -β sites differ from those in groups I and II at position 1 (A versus C), a substitution previously shown by Thornell et al. (77) to decrease CBF binding. MX is unique among sites with a G at position 2, which was also previously shown to decrease CBF binding (77).

Group IV consists of the SS4 site, which has the favorable C

TABLE 2. Core sites used for equilibrium binding analysis[a]

Virus, enhancer, or site[b]	Core site sequence
Consensus sequence	NYGYGGTNN
Moloney MLV, Friend MLV, Moloney MSV, 4070-a, HaMSV, MPSV, Cas-Br-E, NS6MCF, and ABLV	CTGTGGTAA
SL3-3, GrLV, FeLV-B, FeLV-A, and HoLV	CTGTGGTTA
Akv, GAL-SE, GAL-SF, SSV, Ki-MSV, RadLV, N-CL-35, B-CL-11, BL/Ka, FBJ-MSV, RFV-en, and AKR614	CTGTGGTCA
MCF247, MCF13, Tikaut, NZB-x, and NSF-x	CTGTGGTCG
Rauscher MCF and Rauscher SFFV	CTGCGGTGA
MX33 and MX27	CGGTGGTCA
Soule MLV	CTGCGGTCA
TCRα	ATGTGGCTT
TCRγ and TCRδ	CTGTGGTTT
TCRβ	ATGTGGTTT
HA	TTGCGGTTT
SAAB	CTGCGGTTT
SS4	CTGCGGAAG
SS5	CTGTGGAAG
Mo(core)	CTGCCGAAA

[a] Core site sequences from enhancers of MLVs (23, 73), TCRα, -β, -δ, and -γ enhancers (21, 30, 59, 60), and five synthetic sites, i.e., the high-affinity (HA) site identified by Thornell et al. (77), the site identified by selected and amplified binding analysis (SAAB) (43), the SS4 and SS5 sites, and the Moloney core site mutation Mo(core) originally made by Speck et al. (70, 71). The consensus sequence identified by Melnikova et al. (43) is indicated at the top. The boundaries of the core sites are defined by the phosphate contacts made by CBF in the Moloney MLV enhancer (43).
[b] The sites in boldface type represent the names chosen for each site used in the equilibrium binding analysis. Abbreviations: Moloney MSV, Moloney murine sarcoma virus; HaMSV, Harvey MSV; ABLV, Abelson leukemia virus; GrLV, Gross passage A leukemia virus; FeLV-B and FeLV-A, feline leukemia virus, B and A subgroup, respectively; HoLV, Ho wild mouse leukemia virus; GAL-SE and GAL-SF, Gibbon ape leukemia virus, SEATO and San Francisco isolates; SSV, simian sarcoma virus; Ki-MSV, Kirsten MSV; RadLV, radiation-induced leukemia virus; FBJ-MSV, Finkel, Biskis, Jinkins murine osteogenic sarcoma virus; RFV-en, chemically induced endogenous retrovirus from RFM-Un mice; NZB-x, NZB xenotropic MLV; NSF-x, NFS-Th-1 xenotropic leukemia virus; Rauscher SFFV, Rauscher spleen focus-forming virus; MX33 and MX27, endogenous polytropic viruses.

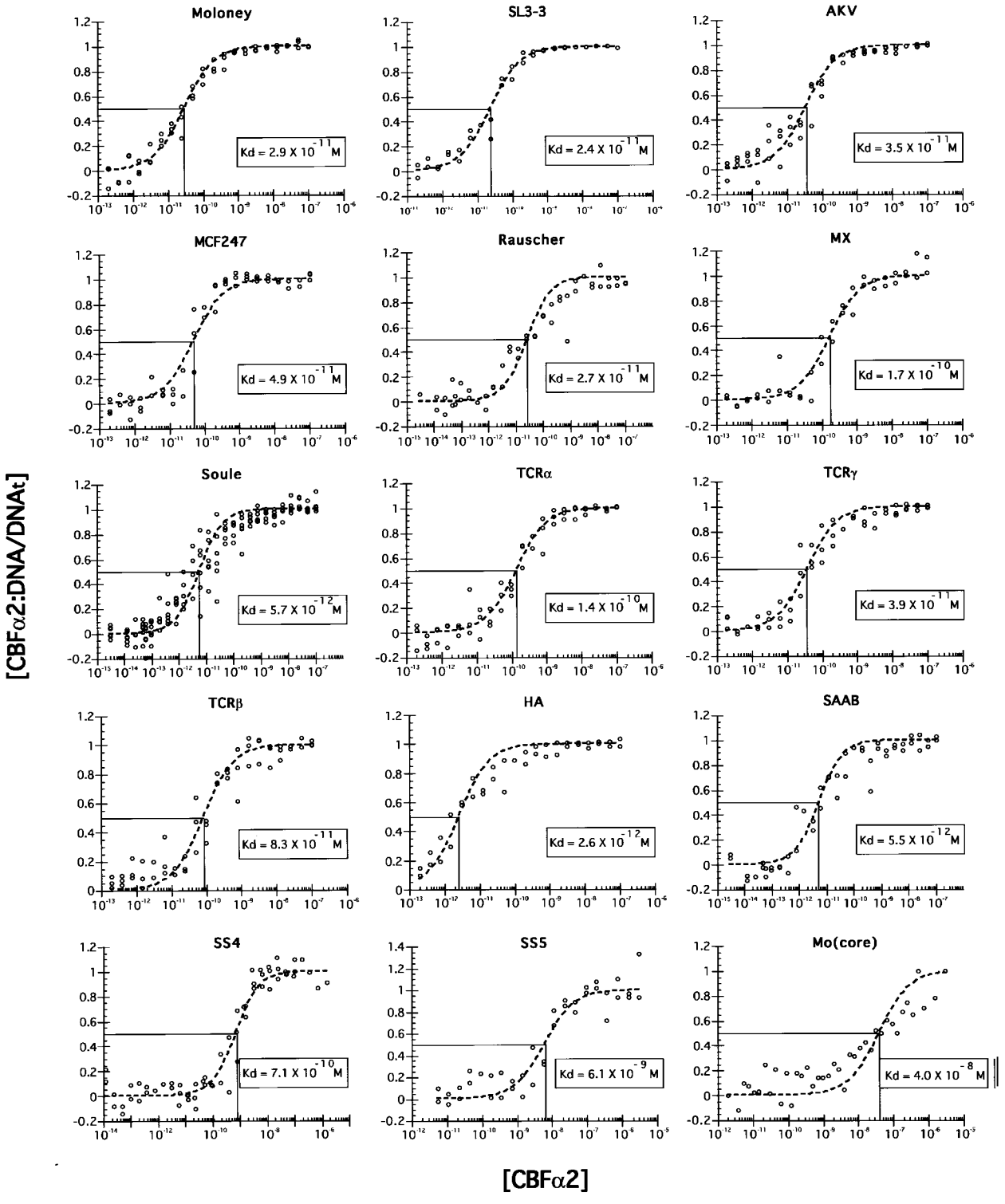

FIG. 3. Equilibrium dissociation constants (Kd) for the CBFα2 Runt domain on representative core sites. EMSAs were performed in the presence of increasing concentrations of the Runt domain indicated on the *x* axis, plotted against the percent Runt domain (CBFα)-DNA complex formation on the *y* axis. For each core site, data from at least two experiments are presented as points plotted on a single graph and fit to a single curve to obtain the K_d.

shared by the highest-affinity core sites in group I (CTGCGG AAG), but an A at position 7 where T is found in most other sites (CTGCGGAAG). We created an even lower affinity site by replacing the C in the fourth position of SS4 with a T to generate SS5 (CTGTGGAAG). Group V consists of the SS5 site. The lowest-affinity site, Mo(core), was the sequence originally introduced into the Moloney MLV enhancer by Speck et al. (70), which significantly altered the disease specificity of

TABLE 3. Summary of equilibrium binding constants

Group	Core site	Sequence	K_d (M)
I	HA	TTGCGGTTA	2.7×10^{-12}
	SAAB	CTGCGGTTT	5.5×10^{-12}
	Soule MLV	CTGCGGTCA	3.5×10^{-12}
II	Moloney MLV	CTGTGGTAA	2.9×10^{-11}
	SL3-3 MLV	CTGTGGTTA	2.4×10^{-11}
	Akv	CTGTGGTCA	3.5×10^{-11}
	MCF247	CTGTGGTCG	4.9×10^{-11}
	Rauscher MCF	CTGCGGTGA	2.7×10^{-11}
	TCRγ	CTGTGGTTT	3.9×10^{-11}
III	TCRα	ATGTGGCTT	1.4×10^{-10}
	MX	CGGTGGTCA	1.7×10^{-10}
	TCRβ	ATGTGGTTT	8.3×10^{-11}
IV	SS4	CTGCGGAAG	9.0×10^{-10}
V	SS5	CTGTGGAAG	6.1×10^{-9}
VI	Mo(core)	CTGCCGTAA	$\geq 4.0 \times 10^{-8}$

Moloney MLV from T-cell leukemia to erythroleukemia. The 2-bp mutation in this site (CTGCCGAAG) presumably disrupts contacts made by CBF to the purine base in the fifth position (82). Weak binding precluded measurement of an accurate K_d value for this core site, and therefore only an approximate K_d is reported. Group VI consists of the Mo(core) site.

The K_d values obtained for the HA and SL3 sites are lower than those reported elsewhere from our laboratory (12, 13). We believe this is due to the presence of the C-terminal KNQHE tag in this particular Runt domain fragment, which may somehow stabilize the overall fold of the isolated domain.

Relationship of CBF affinity and transcriptional activity. To determine whether there is a correlation between the affinity of CBF for different core sites and transcriptional activity in T cells, core sites with a range of affinities for the Runt domain were engineered into the Moloney MLV enhancer, and transcriptional activity was measured in several T-cell lines. One core site from each of groups I to VI was analyzed. Sites were chosen to reduce the possibility of interfering with protein assembly on adjacent sites in the Moloney MLV enhancer. For example, the Soule MLV site (CTGCGGTCA) was chosen to represent group I, since the HA site (TTGCGTTA) has a substitution at position 1 relative to Moloney MLV (CTGTG GTAA) that could theoretically perturb proteins binding to sequences immediately flanking the core site. The Soule MLV site was also deemed preferable to the selected and amplified binding site (SAAB) because it shares an A with Moloney MLV at position 9. The core sites engineered into the Moloney MLV enhancer in order of affinity from highest to lowest are as follows: Soule > SL3-3 > MX > SS4 > SS5 > Mo(core). PCR mutagenesis was used to introduce the selected core sites into both copies of the Moloney MLV direct repeat, which in turn was subcloned into a reporter plasmid containing the firefly luciferase gene (see Material and Methods and Fig. 1). Transcription was analyzed in three T-cell lines; Jurkat, 2017, and D5H3 (Fig. 4). The pattern of transcriptional activity from cell line to cell line was very similar. In general, Moloney MLV enhancers containing the higher-affinity sites (groups I and II) displayed a higher level of transcriptional activity than Moloney MLV enhancers with lower-affinity sites (groups III and VI), but a strict correlation between core site affinity and transcriptional activity was not observed. Specifically, there was not a linear decrease in transcriptional activity that matched the progressive decrease in core site affinity for CBF. For example, the enhancer with the highest-affinity core site (Soule MLV, $K_d = 5.7 \times 10^{-12}$ M), displayed only half the transcriptional activity in all three T-cell lines compared to the enhancer containing the next lowest affinity core site, SL3-3 ($K_d = 2.4 \times 10^{-11}$ M). An even more dramatic deviation was observed with the MX core site ($K_d = 1.7 \times 10^{-10}$ M) from group III, which conferred almost no transcriptional activity in any T-cell line tested. The level of transcription driven by the MX core site was equal to or below that conferred by the lowest-affinity site, Mo(core), despite the fact that the Runt domain affinity for the MX site was approximately 200-fold higher than for Mo(core) ($K_d \geq 4.0 \times 10^{-8}$ M).

Pathogenesis of Moloney MLVs containing altered core sites. We introduced core sites from groups I to VI into the Moloney MLV genome, generated infectious viruses, and analyzed the pathogenicity of these viruses in newborn NFS mice. Virus stocks generated from two or three independent molecular clones for each enhancer mutation were analyzed (Fig. 5 and Table 4). All viruses were leukemogenic, but their pathogenic properties varied. The latent period of disease onset appeared to inversely correlate with the transcriptional activity conferred by these core sites in T cells. The viruses could be divided into two groups with respect to latent period (Fig. 5). Viruses containing high-affinity core sites (Mo:Soule and Mo:SL3-3) that conferred relatively high transcriptional activity in T cells induced disease with significantly shorter latent periods than viruses containing low-affinity sites (Mo:MX, Mo:SS4, Mo:SS5, and Mo:core). The differences in latent periods among the three high-affinity core site viruses (Moloney, Mo:Soule, and Mo:SL3-3) or among the viruses containing low-affinity sites (Mo:MX, Mo:SS4, Mo:SS5, and Mo:core) were not statistically significant by analysis of variance. By this analysis, however, there was a statistically significant difference between the latent periods of disease onset associated with the higher-affinity core site viruses (Moloney, Mo:Soule, and Mo:SL3-3) and the latencies associated with the lower-affinity core site viruses (Mo:MX, Mo:SS4, Mo:SS5, and Mo:core).

Table 4 shows the frequency of each type of hematopoietic neoplasm induced by viruses containing mutations in the enhancer sequence. Moloney viruses containing cores sites from groups I and II (including wild-type Moloney MLV) induced exclusively T-cell lymphomas. Moloney viruses containing the lower-affinity MX core site (group III) induced primarily lymphoblastic lymphomas (12 of 17 neoplasms [71%]). In three additional cases, splenomegaly and lymphadenopathy were predominant features but molecular analysis of the TCRβ and IgH loci detected no rearrangements. Histologically these tumors were poorly differentiated, composed of lymphoblast-like cells with abundant cytoplasm, vesicular chromatin pattern, and prominent nucleoli, with undifferentiated, possibly myeloid blasts in peripheral smears. These cases could represent very early B-cell lymphomas that have not rearranged their IgH alleles, as may be the case in prenatal pre-B-cell lymphomas in Eμ-*myc* and Eμ-*pim*-1 double transgenic mice (79), or they could be lymphomas of lymphoid precursors or stem cells. Further testing will be required to classify these cases definitively.

The Mo:SS4 virus induced two cases of myelogenous leukemia and two of lymphoblastic leukemia (T- or B-cell origin not molecularly determined). The small numbers of mice infected with Mo:SS4 precludes a clear definition of its pathogenicity. Viruses in the groups with the lowest-affinity sites groups V and VI (Mo:SS5 and Mo:core) induce no myeloid tumors, but

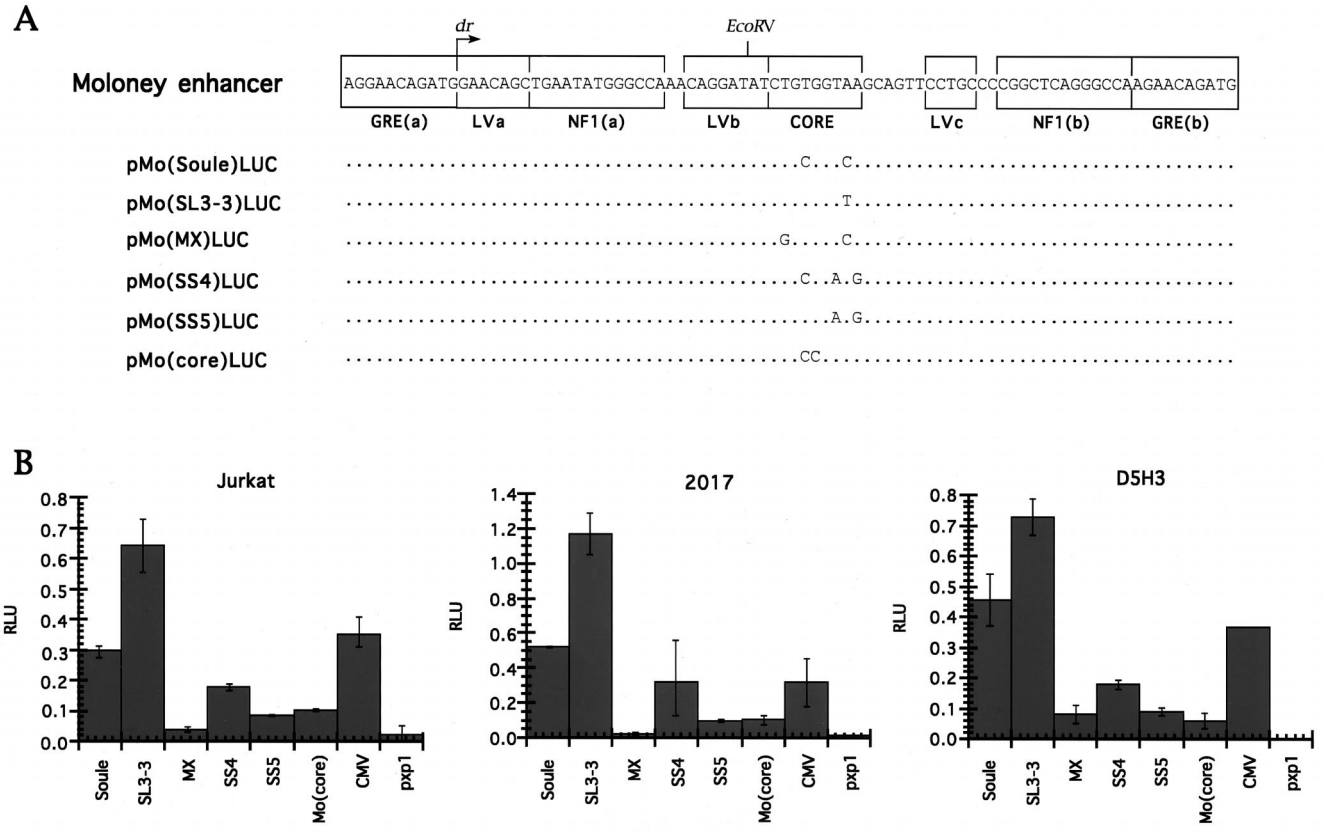

FIG. 4. Effects of different core sites on transcription driven by the Moloney MLV enhancer in T cells. (A) Sequence represents the promoter-distal copy of the direct repeat (*dr*). Core mutations were introduced into both copies of the direct repeat. Binding sites for nuclear factors are boxed. Bases identical to those in the Moloney MLV enhancer are indicated by dots, and capital letters indicate base pair substitutions. (B) Transcriptional activity in Jurkat cells, induced with 1,3-phorbol myristate acetate (1 μg/ml) 24 h posttransfection, 2017 cells, and D5H3 cells. Core sites are arranged in order of decreasing affinity for the Runt domain (from left to right). The absolute luciferase activity was normalized to the protein concentration in each sample (relative luciferase units [RLU] on the *y* axis. Datum points represent the means of three experiments performed on the same day. Error bars represent the standard deviations for the three experiments.

a significant percentage of erythroleukemias. Therefore, T-cell disease specificity appeared to correlate with core site affinity, in that viruses with relatively low-affinity core sites do not maintain the exquisite T-cell disease specificity of Moloney MLV and instead induce a variety of leukemias.

DISCUSSION

CBF is one of many proteins that bind MLV enhancers and one of several transcription factors that bind the core site. Here we show that the affinity of CBF for its DNA-binding site in Moloney MLV correlates with the latent period of disease onset and disease specificity of the virus. Altered Moloney viruses that contain high-affinity CBF binding sites induce predominantly thymic lymphoblastic lymphomas, whereas viruses with lower-affinity CBF binding sites lose the exquisite T-cell disease specificity of Moloney MLV. The results suggest that CBF, which was identified as a candidate host cell transcription factor responsible for the T-cell disease specificity of Moloney MLV (82), may in fact be contributing to the T-cell disease specificity of this virus in vivo. It is also formally possible that we inadvertently created high-affinity binding sites for proteins expressed in hematopoietic cells other than T cells upon introducing low-affinity CBF binding sites into the Moloney MLV enhancer and that this caused alterations in disease specificity.

Although the affinity of CBF for its site appears to correlate with the latent period of disease onset and T-cell disease specificity, it does not do so in a linear fashion. Rather, there appears to be an affinity threshold for inducing T-cell lymphoma following a rapid latent period. The Moloney, Mo:Soule, and Mo:SL3-3 MLVs contain core sites above this affinity threshold and induce exclusively T-cell lymphomas following a short latent period. Mo:MX, Mo:SS4, Mo:SS5, and Mo:core contain core sites below the affinity threshold and induce a mixture of T- and B-cell lymphomas, myeloid leukemias, and erythroleukemias following a longer latent period.

Although there was a rough correlation between CBF affinity and transcriptional activity in T cells, two core sites deviated from this pattern for reasons we do not fully understand. The Soule MLV core site, which is in the group of high-affinity sites (group I), and bound CBF with a sevenfold-higher affinity than the SL3-3 core site, conferred lower levels of transcription to the Moloney MLV enhancer than the SL3-3 site. The difficulty we experienced in measuring a dissociation constant for the Soule MLV site may have caused us to underestimate the K_d, although in no experiments did we measure a K_d for the Soule core site that was higher than that for SL3-3. Another possible explanation for this discrepancy is that the mutation we introduced in the Moloney enhancer to generate the Soule MLV site may have altered binding of other proteins to the enhancer. In this regard, we note that the C at position 8 of the Soule site is shared by the Akv virus. In other studies, it has been demonstrated that the C at position 8 in Akv, when used

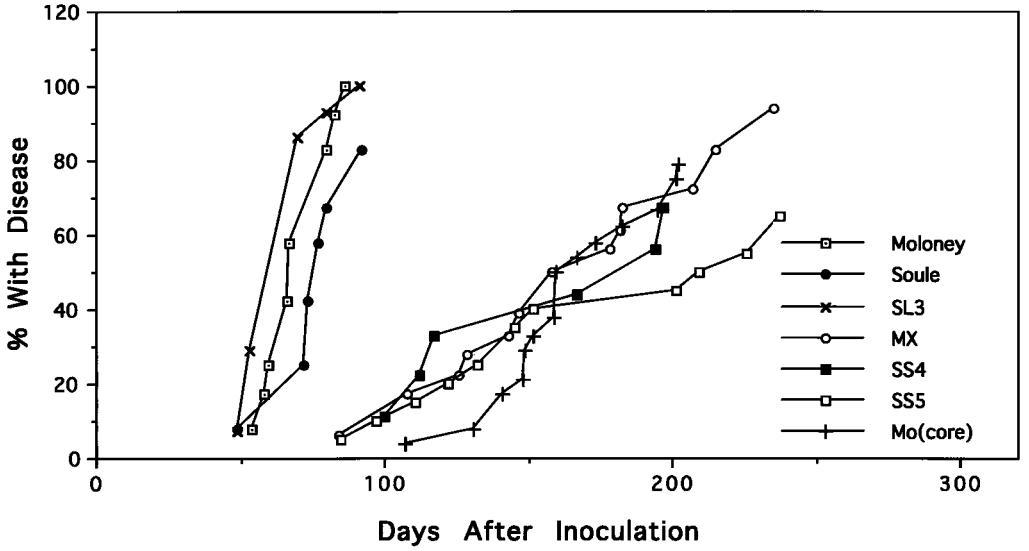

FIG. 5. Leukemia induction in NFS mice. Leukemia induction as a function of time, following injection of newborn NFS mice with the wild-type Moloney virus and viruses containing altered core sites.

to replace the T at that same position in the SL3-3 virus, reduces transcription from the SL3-3 enhancer in T cells and attenuates pathogenesis (6, 47). Similarly, this alteration in the Moloney MLV enhancer, while not significantly affecting CBF affinity (compare the Moloney MLV and Akv sites in Table 3), may nevertheless be responsible for reducing transcriptional activity in T cells. Our experiments support the hypothesis put forth by Zaiman et al. (86), that the T-versus-C difference in the SL3-3 and Akv core sites is most likely influencing transcription and pathogenesis through some protein other than (or in addition to) CBF, since the affinities of CBF for the SL3-3 and Akv sites are very similar.

The other unexpected result was that obtained with the endogenous polytropic and modified polytropic MX viruses. When this core site was introduced into the Moloney MLV enhancer, it dramatically reduced transcription in T cells, as much as or even more than the Mo(core) mutation that essentially eliminates CBF binding. Again, the data suggest that the sequence alteration impacted on some other protein binding to the enhancer in T cells. The Ets proteins, for example, bind the adjacent LVb site 5′ to the core site. However, preliminary data (not shown) indicated that Ets-1 binding was not appreciably affected by the MX mutation. The MX site also has a C at position 7, similar to Soule and Akv. Pathogenicity was affected, in that there was increased heterogeneity in tumor phenotype and latency was prolonged.

We note that most MLVs contain relatively high-affinity CBF binding sites (groups I and II). Only the endogenous polytropic and modified polytropic viruses (MX27 and MX33) contain low-affinity CBF sites. The endogenous polytropic viruses are replication defective and serve as *env* donors for recombinant MCF viruses, but the enhancers from these vi-

TABLE 4. Latent period of disease induction and types of leukemia and lymphoma cause by wild-type and mutant Moloney viruses

Virus	Core site K_d (M)	No. positive/no. inoculated[a]	Avg latent period (days)[b]	No. of tumors (%)[c]					
				Lymphoblastic lymphoma			Myelogenous leukemia	Erythroleukemia	Other
				T-cell Lymphoma	B-cell lymphoma	Untyped[d]			
Moloney	2.9×10^{-11}	12/12	71 (11)	12 (100)	0	0	0	0	0
Mo:Soule	3.5×10^{-12}	10/12	76 (12)	10 (100)	0	0	0	0	0
Mo:SL3-3	2.4×10^{-11}	14/14	64 (12)	13 (100)	0	0	0	0	1[e]
Mo:MX	1.7×10^{-10}	17/18	166 (46)	5 (36)	2 (14)	5 (36)	1 (6)[e]	1 (6)	3[f]
Mo:SS4	9.0×10^{-10}	6/9	148 (43)	0	0	2 (50)	2 (50)	0	2[e]
Mo:SS5	6.1×10^{-9}	14/20	163 (52)	7 (64)	1 (9)	1 (9)	0	2 (18)	2[e]
Mo:core[g]	$>4.0 \times 10^{-8}$	19/24	162 (26)	5 (28)	0	0	0	11 (61)	1[e], 2[h]

[a] Number of mice positive by 9 months postinoculation, at which point the experiment was terminated, to the number of mice inoculated.
[b] Average latent period is calculated from animals with disease that were sacrificed or found dead. Standard deviations are in parentheses.
[c] Lineage typing of cases of lymphoblastic lymphoma with no thymic involvement were based on TCRβ and IgH rearrangements detected in Southern blots of spleen or lymph node DNA. The percentage of each lymphoma or leukemia relative to all diagnosed disease is indicated in parentheses.
[d] Nonthymic lymphoma, not tested for TCRβ or IgH rearrangements.
[e] Dead, no diagnosis.
[f] Non-thymic, non-T, non-B by TCRβ and IgH rearrangement. Morphologically lymphoblastic but poorly differentiated, with undifferentiated blasts in peripheral smears.
[g] Data from Speck et al. (70). Molecular analysis of TCRβ and IgH rearrangements not performed.
[h] Lymphoma plus erythroleukemia (11%).

ruses are not found in infectious MLVs (73). Thus, it appears that CBF has the potential to act on most MLV enhancers in vivo.

The expression pattern of *Cbfa2*, which encodes the CBFα subunit originally purified from thymus tissue (82), may shed some light on why the lowest-affinity core sites in the Moloney MLV enhancer [SS5 and Mo(core)] tend to shift disease specificity toward erythroleukemia. *Cbfa2* is highly expressed in c-*kit*$^+$ CD34$^+$ fetal liver hematopoietic stem cells and in bone marrow (11, 15, 50). Expression remains high in the thymus and in some (if not all) myeloid lineages but appears to be rapidly downregulated in both the primitive and definitive erythroid lineages (11, 50, 65, 68). Thus, CBF may not be important for Moloney MLV replication in cells of the erythroid lineage. Low-affinity core sites may selectively impair transcription of the Moloney MLV genome in lymphocytes and in myeloid lineages, but not in erythroid progenitors, hence shifting the distribution of leukemias toward the erythroid lineage.

ACKNOWLEDGMENTS

We thank Barbara Graves for advice in measuring dissociation constants and the members of Bill Green's laboratory for help in generating infectious viruses. We also thank Torgny Fredrickson for histopathology consultation, Sandy Morse and Sisir Chattopadhyay for critical comments, and Zohreh Nagashfar for technical assistance. We also gratefully acknowledge Sisir Chattopadhyay for providing DNA probes.

This work was supported in part by Public Health Service grants R01 CA58343 and CA75611 (awarded to N.A.S.) and by contract N01-AI-45203 at MA Bioservices, Inc., Rockville, Md. A.F.L. was supported by a Cancer Biology Training Grant CA09658. W.R.G. is supported by CA 69525. N.A.S. is a Leukemia Society of American Scholar.

REFERENCES

1. **Amtoft, H. W., A. B. Sorensen, C. Bareil, J. Schmidt, A. Luz, and F. S. Pedersen.** 1997. Stability of AML1 (core) site enhancer mutations in T lymphomas induced by attenuated SL3-3 murine leukemia virus mutants. J. Virol. **71:**5080–5087.
2. **Bae, S.-C., E. Takahashi, Y. W. Zhang, E. Ogawa, K. Shigesada, Y. Namba, M. Satake, and Y. Ito.** 1995. Cloning, mapping and expression of *PEBP2αC*, a third gene encoding the mammalian Runt domain. Gene **159:**245–248.
3. **Bae, S. C., Y. Yamaguchi-Iwai, E. Ogawa, M. Maruyama, M. Inuzuka, H. Kagoshima, K. Shigesada, M. Satake, and Y. Ito.** 1993. Isolation of PEBP2αB cDNA representing the mouse homolog of human acute myeloid leukemia gene, *AML1*. Oncogene **8:**809–814.
4. **Baltimore, D.** 1970. RNA-dependent DNA polymerase in virions of RNA tumor viruses. Nature **226:**1209–1211.
5. **Bitter, M. A., M. M. LeBeau, J. D. Rowley, R. A. Larson, H. M. Golomb, and J. W. Vardiman.** 1987. Association between morphology, karyotype, and clinical features in myeloid leukemias. Human Pathol. **18:**211–225.
6. **Boral, A. L., S. A. Okenquist, and J. Lenz.** 1989. Identification of the SL3-3 virus enhancer core as a T-lymphoma cell-specific element. J. Virol. **63:**76–84.
7. **Bowie, J. U., and R. T. Sauer.** 1989. Identification of C-terminal extensions that protect proteins from intracellular proteolysis. J. Biol. Chem. **264:**7596–7602.
8. **Cameron, S., D. S. Taylor, E. C. TePas, N. A. Speck, and B. Mathet-Prevot.** 1994. Identification of a critical regulatory site in the human interleukin-3 promoter by in vivo footprinting. Blood **83:**2851–2859.
9. **Chatis, P. A., C. A. Holland, J. W. Hartley, W. P. Rowe, and N. Hopkins.** 1983. Role for the 3′ end of the genome in determining disease specificity of Friend and Moloney murine leukemia viruses. Proc. Natl. Acad. Sci. USA **80:**4408–4411.
10. **Chatis, P. A., C. A. Holland, J. E. Silver, T. N. Fredrickson, N. Hopkins, and J. W. Hartley.** 1984. A 3′ end fragment encompassing the transcriptional enhancer of nondefective Friend virus confers erythroleukemogenicity on Moloney murine leukemia virus. J. Virol. **52:**248–259.
11. **Corsetti, M. T., and F. Calabi.** 1997. Lineage- and stage-specific expression of Runt box polypeptides in primitive and definitive hematopoiesis. Blood **89:**2359–2368.
12. **Crute, B. E., A. F. Lewis, Z. Wu, J. H. Bushweller, and N. A. Speck.** 1996. Biochemical and biophysical properties of the CBFα2 (AML1) DNA-binding domain. J. Biol. Chem. **271:**26251–26260.
13. **Crute, B. E., Y.-Y. Tang, X. Huang, J. J. Kelley III, K. L. Hartman, T. Laue, N. A. Speck, and J. H. Bushweller.** Biophysical characterization of interactions between the core binding factor α and β subunits and DNA. Submitted for publication.
14. **de Wet, J. R., K. V. Wood, M. DeLuca, D. R. Helinski, and S. Subramani.** 1987. Firefly luciferase gene: structure and expression in mammalian cells. Mol. Cell. Biol. **7:**725–737.
15. **Erickson, P. F., G. Dessev, R. S. Lasher, G. Philips, M. Robinson, and H. A. Drabkin.** 1996. ETO and AML1 phosphoproteins are expressed in CD34+ hematopoietic progenitors: implications for t(8;21) leukemogenesis and monitoring residual disease. Blood **88:**1813–1823.
16. **Erman, B., M. Cortes, B. S. Nikolajczyk, N. A. Speck, and R. Sen.** 1998. ETS-core binding factor: a common composite motif in antigen receptor gene enhancers. Mol. Cell. Biol. **18:**1322–1330.
17. **Ethelberg, S., B. Hallberg, J. Lovmand, J. Schmidt, A. Luz, T. Grundstrom, and F. S. Pedersen.** 1997. Second-site proviral enhancer alterations in lymphomas induced by enhancer mutants of SL3-3 murine leukemia virus: negative effect of nuclear factor 1 binding site. J. Virol. **71:**1196–1206.
18. **Ethelberg, S., J. Lovmand, J. Schmidt, A. Luz, and F. S. Pedersen.** 1997. Increased lymphomagenicity and restored disease specificity of AML1 site (core) mutant SL3-3 murine leukemia virus by a second-site enhancer variant evolved in vivo. J. Virol. **71:**7273–7280.
19. **Frank, R., J. Zhang, H. Uchida, S. Meyers, S. W. Hiebert, and S. D. Nimer.** 1995. The AML1/ETO fusion protein blocks transactivation of the GM-CSF promoter by AML1B. Oncogene **11:**2667–2674.
20. **Gamou, T., E. Kitamura, F. Hosoda, K. Shimizu, K. Shinohara, Y. Hayashi, T. Nagese, Y. Yokoyama, and M. Ohki.** 1998. The partner gene of *AML1* in t(16;21) myeloid malignancies is a novel member of the *MTG8(ETO)* family. Blood **91:**4028–4037.
21. **Giese, K., C. Kingsley, J. R. Kirshner, and R. Grosschedl.** 1995. Assembly and function of a TCRα enhancer complex is dependent on LEF-1-induced DNA binding and multiple protein-protein interactions. Genes Dev. **9:**995–1008.
22. **Golemis, E., Y. Li, T. N. Fredrickson, J. W. Hartley, and N. Hopkins.** 1989. Distinct segments in the enhancer region collaborate to specify the type of leukemia induced by nondefective Friend and Moloney viruses. J. Virol. **63:**328–337.
23. **Golemis, E., N. A. Speck, and N. Hopkins.** 1990. Alignment of U3 region sequences of mammalian type C viruses: identification of highly conserved motifs and implications for enhancer design. J. Virol. **64:**534–542.
24. **Golub, T. R., G. F. Barker, S. K. Bohlander, S. Hiebert, D. C. Ward, P. Bray-Ward, E. Morgan, S. C. Raimondi, J. D. Rowley, and D. G. Gilliland.** 1995. Fusion of the *TEL* gene on 12p13 to the *AML1* gene on 21q22 in acute lymphoblastic leukemia. Proc. Natl. Acad. Sci. USA **92:**4917–4921.
25. **Gould, S. J., and S. Subramani.** 1989. Firefly luciferase as a tool in molecular and cell biology, p. 9.6.10–9.6.14. *In* F. M. Ausubel, R. Brent, R. E. Kingston, D. D. Moore, J. G. Seidman, J. A. Smith, and K. Struhl (ed.), Current protocols in molecular biology, vol. 2. Greene Publishing Associates and Wiley-Interscience, New York, N.Y.
26. **Gross-Belland, M., P. Oudet, and P. Chambon.** 1973. Isolation of high molecular weight DNA from mammalian cells. Eur. J. Biochem. **36:**32–37.
27. **Hallberg, B., J. Schmidt, A. Luz, F. S. Pedersen, and T. Grundstrom.** 1991. SL3-3 enhancer factor 1 transcriptional activators are required for tumor formation by SL3-3 murine leukemia virus. J. Virol. **65:**4177–4181.
28. **Hallberg, B., A. Thornell, M. Holm, and T. Grundstrom.** 1992. SEF1 binding is important for T cell specific enhancers of genes for T cell receptor-CD3 subunits. Nucleic Acids Res. **20:**6495–6499.
29. **Hedrick, S. M., R. N. Germain, M. Bevan, M. Dorf, I. Engel, P. Fink, N. Gascoigne, E. Heber-Katz, J. Kapp, Y. Kaufmann, J. Kaye, F. Melchers, C. Pierce, R. Schwartz, C. Sorenson, M. Taniguchi, and M. M. Davis.** 1985. Rearrangement and transcription of a T-cell receptor B-chain gene in different T cell subsets. Proc. Natl. Acad. Sci. USA **82:**531–535.
30. **Hsiang, Y. H., D. Spencer, S. Wang, N. A. Speck, and D. H. Raulet.** 1993. The role of viral "core" motif-related sequences in regulating T cell receptor γ and δ gene expression. J. Immunol. **150:**3905–3916.
31. **Ishimoto, A., M. Takimoto, A. Adachi, M. Kakuyama, S. Kato, K. Kakimi, K. Fukuoka, T. Ogiu, and M. Matsuyama.** 1987. Sequences responsible for erythroid and lymphoid leukemia in the long terminal repeats of Friend-mink cell focus-forming and Moloney murine leukemia viruses. J. Virol. **61:**1861–1866.
32. **Jonsen, M. D., J. M. Petersen, Q.-P. Xu, and B. J. Graves.** 1996. Characterization of cooperative function of inhibitory sequences in Ets-1. Mol. Cell. Biol. **16:**2065–2073.
33. **Kamachi, Y., E. Ogawa, M. Asano, S. Ishida, Y. Murakami, M. Satake, Y. Ito, and K. Shigesada.** 1990. Purification of a mouse nuclear factor that binds to both the A and B cores of the polyomavirus enhancer. J. Virol. **64:**4808–4819.
34. **Kingston, R. E.** 1989. Transfection of DNA into eukaryotic cells, p. 9.1.1–9.1.3. *In* F. M. Ausubel, R. Brent, R. E. Kingston, D. D. Moore, J. G. Seidman, J. A. Smith, and K. Struhl (ed.), Current protocols in molecular biology, vol. 2. Greene Publishing Associates and Wiley-Interscience, New York, N.Y.
35. **Lang, R. B., L. W. Stanton, and K. B. Marcu.** 1982. On immunoglobulin

heavy chain switching: two γ2b genes are rearranged via switch sequences in MPC-11 cells but only one is expressed. Nucleic Acids Res. **10:**611–630.
36. **Lenz, J., D. Celander, R. L. Crowther, R. Patarca, D. E. Perkins, and W. A. Haseltine.** 1984. Determination of the leukaemogenicity of a murine retrovirus by sequences within the long terminal repeat. Nature (London) **308:** 467–470.
37. **Levanon, D., V. Negreanu, Y. Bernstein, I. Bar-Am, L. Avivi, and Y. Groner.** 1994. *AML1*, *AML2*, and *AML3*, the human members of the runt domain gene-family: cDNA structure, expression, and chromosomal localization. Genomics **23:**425–432.
38. **Li, Y., E. Golemis, J. W. Hartley, and N. Hopkins.** 1987. Disease specificity of nondefective Friend and Moloney murine leukemia viruses is controlled by a small number of nucleotides. J. Virol. **61:**696–700.
39. **Liu, P., S. A. Tarle, A. Hajra, D. F. Claxton, P. Marlton, M. Freedman, M. J. Siciliano, and F. S. Collins.** 1993. Fusion between transcription factor CBFβ/PEBP2β and a myosin heavy chain in acute myeloid leukemia. Science **261:**1041–1044.
40. **Losardo, J. E., A. L. Boral, and J. Lenz.** 1990. Relative importance of elements within the SL3-3 virus enhancer for T-cell specificity. J. Virol. **64:**1756–1763.
41. **Manley, N. R., M. A. O'Connell, P. A. Sharp, and N. Hopkins.** 1989. Nuclear factors that bind to the enhancer region of nondefective Friend murine leukemia virus. J. Virol. **63:**4210–4223.
42. **McLean, T. W., S. Ringold, D. Neuberg, K. Stegmaier, R. Tantravahi, J. Ritz, H. P. Koeffler, S. Takeuchi, J. W. Janssen, T. Seriu, C. R. Bartram, S. E. Sallan, D. G. Gilliland, and T. R. Golub.** 1996. TEL/AML-1 dimerizes and is associated with a favorable outcome in childhood acute lymphoblastic leukemia. Blood **88:**4252–4258.
43. **Melnikova, I., B. E. Crute, S. Wang, and N. A. Speck.** 1993. Sequence specificity of the core-binding factor. J. Virol. **67:**2408–2411.
44. **Mercurio, F., and M. Karin.** 1989. Transcription factors AP-3 and AP-2 interact with the SV40 enhancer in a mutually exclusive manner. EMBO J. **8:**1455–1460.
45. **Milla, M. E., B. M. Brown, and R. T. Sauer.** 1993. P22 arc repressor: enhanced expression of unstable mutants by addition of polar C-terminal sequences. Protein Sci. **2:**2198–2205.
46. **Miyoshi, H., K. Shimizu, T. Kozu, N. Maseki, Y. Kaneko, and M. Ohki.** 1991. t(8;21) breakpoints on chromosome 21 in acute myeloid leukemia are clustered within a limited region of a single gene, *AML1*. Proc. Natl. Acad. Sci. USA **88:**10431–10434.
47. **Morrison, H. L., B. Soni, and J. Lenz.** 1995. Long terminal repeat enhancer core sequences in proviruses adjacent to c-*myc* in T-cell lymphomas induced by a murine retrovirus. J. Virol. **69:**446–455.
48. **Niki, M., H. Okada, H. Takano, J. Kuno, K. Tani, H. Hibino, S. Asano, Y. Ito, M. Satake, and T. Noda.** 1997. Hematopoiesis in the fetal liver is impaired by targeted mutagenesis of a gene encoding a non-DNA binding subunit of the transcription factor, polyomavirus enhancer binding protein 2/core binding factor. Proc. Natl. Acad. Sci. USA **94:**5697–5702.
49. **Nordeen, S. K.** 1988. Luciferase reporter gene vectors for analysis of promoters and enhancers. BioTechniques **6:**454–457.
50. **North, T. E., T.-L. Gu, T. Stacy, Q. Wang, L. Howard, M. Binder, M. Marín-Padilla, and N. A. Speck.** *Cbfa2* is required for the formation of intraaortic hematopoietic clusters. Development, in press.
51. **Nuchprayoon, I., S. Meyers, L. M. Scott, J. Suzow, S. Hiebert, and A. D. Friedman.** 1994. PEBP2/CBF, the murine homolog of the human myeloid AML1 and PEBP2β/CBFβ proto-oncoproteins, regulates the murine myeloperoxidase and neutrophil elastase genes in immature myeloid cells. Mol. Cell. Biol. **14:**5558–5568.
52. **Nucifora, G., C. R. Begy, P. Erickson, H. A. Drabkin, and J. D. Rowley.** 1993. The 3;21 translocation in myelodysplasia results in a fusion transcript between the AML1 gene and the gene for EAP, a highly conserved protein associated with the Epstein-Barr virus small RNA EBER 1. Proc. Natl. Acad. Sci. USA **90:**7784–7788.
53. **Nucifora, G., C. R. Begy, H. Kobayashi, D. Roulston, D. Claxton, J. Pedersen-Bjergaard, E. Parganas, J. N. Ihle, and J. D. Rowley.** 1994. Consistent intergenic splicing and production of multiple transcripts between AML1 at 21q22 and unrelated genes at 3q26 in (3;21)(q26;q22) translocations. Proc. Natl. Acad. Sci. USA **91:**4004–4008.
54. **Ogawa, E., M. Inuzuka, M. Maruyama, M. Satake, M. Naito-Fujimoto, Y. Ito, and K. Shigesada.** 1993. Molecular cloning and characterization of PEBP2β, the heterodimeric partner of a novel Drosophila runt-related DNA binding protein PEBP2α. Virology **194:**314–331.
55. **Ogawa, E., M. Maruyama, H. Kagoshima, M. Inuzuka, J. Lu, M. Satake, K. Shigesada, and Y. Ito.** 1993. PEBP2/PEA2 represents a new family of transcription factor homologous to the products of the Drosophila *runt* and the human *AML1* gene. Proc. Natl. Acad. Sci. USA **90:**6859–6863.
56. **Okuda, T., J. van Deursen, S. W. Hiebert, G. Grosveld, and J. R. Downing.** 1996. AML1, the target of multiple chromosomal translocations in human leukemia, is essential for normal fetal liver hematopoiesis. Cell **84:**321–330.
57. **Parsell, D. A., and R. T. Sauer.** 1988. The structural stability of a protein is an important determinant of its proteolytic susceptibility in *Escherichia coli*. J. Biol. Chem. **264:**7590–7595.
58. **Parsell, D. A., K. R. Silber, and R. T. Sauer.** 1990. Carboxy-terminal determinants of intracellular protein degradation. Genes Dev. **4:**277–286.
59. **Prosser, H. M., D. Wotton, A. Gegonne, J. Ghysdael, S. Wang, N. A. Speck, and M. J. Owen.** 1992. A novel phorbol ester response element within the human T cell receptor β enhancer. Proc. Natl. Acad. Sci. USA **89:**9934–9938.
60. **Redondo, J. M., J. L. Pfohl, C. Hernandez-Munain, S. Wang, N. A. Speck, and M. Krangel.** 1992. Indistinguishable nuclear factor binding to functional core sites of the T-cell receptor δ and murine leukemia virus enhancers. Mol. Cell. Biol. **12:**4817–4823.
61. **Romana, S. P., M. Mauchauffe, M. Le Coniat, I. Chumakow, D. Le Paslier, R. Berger, and O. A. Bernard.** 1995. The t(12;21) of acute lymphoblastic leukemia results in a tel-AML1 gene fusion. Blood **85:**3662–3670.
62. **Romana, S. P., H. Poirel, M. Leconiat, M.-A. Flexor, M. Mauchauffé, P. Jonveaux, E. A. Macintyre, R. Berger, and O. A. Bernard.** 1995. High frequency of t(12;21) in childhood B-lineage acute lymphoblastic leukemia. Blood **86:**4263–4269.
63. **Rowe, W. P., W. E. Pugh, and J. W. Hartley.** 1970. Plaque assay techniques for murine leukemia viruses. Virology **42:**1136–1139.
64. **Sasaki, K., H. Yagi, R. T. Bronson, K. Tominaga, T. Matsunashi, K. Deguchi, Y. Tani, T. Kishimoto, and T. Komori.** 1996. Absence of fetal liver hematopoiesis in transcriptional co-activator, core binding factor β (*Cbfb*) deficient mice. Proc. Natl. Acad. Sci. USA **93:**12359–12363.
65. **Satake, M., S. Nomura, Y. Yamaguchi-Iwai, Y. Takahama, Y. Hashimoto, M. Niki, K. Yukihiko, and Y. Ito.** 1995. Expression of the Runt domain encoding *PEBP2*α genes in T cells during thymic development. Mol. Cell. Biol. **15:** 1662–1670.
66. **Shurtleff, S. A., A. Buijs, F. G. Behm, J. E. Rubnitz, S. C. Raimondi, M. L. Hancock, G. C.-F. Chan, C.-H. Pui, G. Grosveld, and J. R. Downing.** 1995. TEL/AML1 fusion resulting from a cryptic t(12;21) is the most common genetic lesion in pediatric ALL and defines a subgroup of patients with an excellent prognosis. Leukemia **9:**1985–1989.
67. **Shurtleff, S. A., S. Meyers, S. W. Hiebert, S. C. Raimondi, D. R. Head, C. L. Willman, S. Wolman, M. L. Slovak, A. J. Carroll, F. Behm, M. G. Hulshof, T. A. Motroni, T. Okuda, P. Liu, F. S. Collins, and J. R. Downing.** 1995. Heterogeneity in CBFB/MYH11 fusion messages encoded by the inv(16)(p13q22) and the t(16;16)(p13;q22) in acute myelogenous leukemia. Blood **85:**3695–3703.
68. **Simeone, A., A. Daga, and F. Calabi.** 1995. Expression of *runt* in the mouse embryo. Dev. Dyn. **203:**61–70.
69. **Speck, N. A., and D. Baltimore.** 1987. Six distinct nuclear factors interact with the 75-base-pair repeat of the Moloney murine leukemia virus enhancer. Mol. Cell. Biol. **7:**1101–1110.
70. **Speck, N. A., B. Renjifo, E. Golemis, T. N. Fredrickson, J. W. Hartley, and N. Hopkins.** 1990. Mutation of the core or adjacent LVb elements of the Moloney murine leukemia virus enhancer alters disease specificity. Genes Dev. **4:**233–242.
71. **Speck, N. A., B. Renjifo, and N. Hopkins.** 1990. Point mutations in the Moloney murine leukemia virus enhancer identify a lymphoid-specific viral core motif and 1,3-phorbol myristate acetate-inducible element. J. Virol. **64:**543–550.
72. **Stewart, M., A. Terry, M. Hu, M. O'Hara, K. Blyth, E. Baxter, E. Cameron, D. E. Onions, and J. C. Neil.** 1997. Proviral insertions induce the expression of bone-specific isoforms of PEBP2αA (*CBFA1*): evidence for a new myc collaborating oncogene. Proc. Natl. Acad. Sci. USA **94:**8646–8651.
73. **Stoye, J. P., and J. M. Coffin.** 1987. The four classes of endogenous murine leukemia virus: structural relationships and potential for recombination. J. Virol. **61:**2659–2669.
74. **Studier, F. W., A. H. Rosenberg, J. J. Dunn, and J. W. Dubendorff.** 1990. Use of T7 RNA polymerase to direct expression of cloned genes. Methods Enzymol. **185:**60–89.
75. **Sun, W., M. O'Connell, and N. A. Speck.** 1993. Characterization of a protein that binds multiple sequences in mammalian type C retrovirus enhancers. J. Virol. **67:**1976–1986.
76. **Takahashi, A., M. Satake, Y. Yamaguchi-Iwai, S.-C. Bae, J. Lu, M. Maruyama, Y. W. Zhang, H. Oka, N. Arai, K. Arai, and Y. Ito.** 1995. Positive and negative regulation of granulocyte-macrophage colony-stimulating factor (GM-CSF) promoter activity by AML1-related transcription factor, PEBP2. Blood **86:**607–616.
77. **Thornell, A., B. Hallberg, and T. Grundstrom.** 1991. Binding of SL3-3 enhancer factor 1 transcriptional activators to viral and chromosomal enhancer sequences. J. Virol. **65:**42–50.
78. **Thornell, A., B. Hallberg, and T. Grundstrom.** 1988. Differential protein binding in lymphocytes to a sequence in the enhancer of the mouse retrovirus SL3-3. Mol. Cell. Biol. **8:**1625–1637.
79. **Verbeek, S., M. van Lohuizen, M. van der Valk, J. Domen, G. Kraal, and A. Berns.** 1991. Mice bearing the Eμ-*myc* and Eμ-*pim*-1 transgenes develop pre-B-cell leukemia prenatally. Mol. Cell. Biol. **11:**1176–1179.
80. **Wang, Q., T. Stacy, M. Binder, M. Marín-Padilla, A. H. Sharpe, and N. A. Speck.** 1996. Disruption of the *Cbfa2* gene causes necrosis and hemorrhaging

in the central nervous system and blocks definitive hematopoiesis. Proc. Natl. Acad. Sci. USA **93:**3444–3449.

81. **Wang, Q., T. Stacy, J. D. Miller, A. F. Lewis, X. Huang, J.-C. Bories, J. H. Bushweller, F. W. Alt, M. Binder, M. Marín-Padilla, A. Sharpe, and N. A. Speck.** 1996. The CBFβ subunit is essential for CBFα2 (AML1) function in vivo. Cell **87:**697–708.
82. **Wang, S., and N. A. Speck.** 1992. Purification of core-binding factor, a protein that binds the conserved core site in murine leukemia virus enhancers. Mol. Cell. Biol. **12:**89–102.
83. **Wang, S., Q. Wang, B. E. Crute, I. N. Melnikova, S. R. Keller, and N. A. Speck.** 1993. Cloning and characterization of subunits of the T-cell receptor and murine leukemia virus enhancer core-binding factor. Mol. Cell. Biol. **13:**3324–3339.
84. **Wargnier, A., S. Legros-Maida, R. Bosselut, J. F. Bourge, C. Lafaurie, C. J. Ghysdael, M. Sasportes, and P. Paul.** 1995. Identification of human granzyme B promoter regulatory elements interacting with activated T-cell-specific proteins: implication of Ikaros and CBF binding sites in promoter activation. Proc. Natl. Acad. Sci. USA **92:**6930–6934.
85. **Weiss, R., N. Teich, H. Varmus, and J. Coffin (ed.).** 1982. RNA tumor viruses, vol. 1. Cold Spring Harbor Laboratory, Cold Spring Harbor, N.Y.
86. **Zaiman, A. L., A. F. Lewis, B. E. Crute, N. A. Speck, and J. Lenz.** 1995. Transcriptional activity of core binding factor α (AML1) and β subunits on murine leukemia virus enhancer cores. J. Virol. **68:**2898–2906.
87. **Zhang, D. E., K. Fujioka, C. J. Hetherington, L. H. Shapiro, H. M. Chen, A. T. Look, and D. G. Tenen.** 1994. Identification of a region which directs the monocytic activity of the colony-stimulating factor 1 (macrophage colony-stimulating factor) receptor promoter and binds PEBP2/CBF (AML1). Mol. Cell. Biol. **14:**8085–8095.